ORIGINAL PAPER

The engine mission simulation system: coupled simulation of aircraft and engine in the mission

Jonas Remiger[1] · Marcel Stößel[1] · Dragan Kožulović[1] · Reinhard Niehuis[1] · Michael Krummenauer[2]

Abstract

When designing future aircraft, the entire system including airframe, propulsion system, energy management and mission control must be considered in a coupled approach at an early design stage. To model and study this complex interaction, the Engine Mission Simulation System (EMSS) environment was created in cooperation with the Bundeswehr Technical Center for Aircraft and Aircraft Equipment. EMSS is intended to serve as a digital, flying test bed at the Institute of Jet Propulsion for the rapid and low-cost evaluation of new concepts for propulsion and power supply systems for new and legacy aircraft designs. This tool chain allows a detailed engine simulation under consideration of its flight condition while using an external propulsion and power control system. First, the software architecture of EMSS is discussed, which involves a propulsion simulation in NPSS® coupled with the X-Plane 11 flight simulator via MATLAB®/Simulink®. The aircraft itself is modeled as a six degrees of freedom simulation using the blade element theory, allowing both complex flight maneuvers and unusual aircraft to be easily simulated. The EMSS achieves real-time capability and enables user-friendly pre-design as well as quick trend detection through the ability to perform focused parametric studies. To evaluate the accuracy of the system's results, the engine model used is validated against experimental data. Subsequently, the aerodynamic characteristics of the aircraft model are verified with a CFD simulation. Finally, a parametric study is used to demonstrate the mission as well as propulsion evaluation capabilities of the Engine Mission Simulation System.

List of symbols

Symbols

δ	Power lever angle
F_N	Net thrust
k	Factor
m	Mass flow
$N1$	Low pressure spool speed
$N2$	High pressure spool speed
T	Temperature

Subscripts

041	Parameter at turbine entry
c	Corrected value

cmd	Commanded value
ff	Fuel mass flow
lim	Limiter
max	Maximum allowable value
$swtch$	Switch/option
Thr	Thrust

Acronyms

BPR	Bypass Ratio
EMSS	Engine Mission Simulation System
FAA	Federal Aviation Administration
FCS	Flight Control System
NASA	National Aeronautics and Space Administration
NPSS	Numerical Propulsion System Simulation
OPR	Overall Pressure Ratio
UAV	Unmanned Aerial Vehicle
UDP	User Datagram Protocol
WTD 61	Bundeswehr Technical Center for Aircraft and Aircraft Equipment

✉ Jonas Remiger
jonas.remiger@unibw.de

1 Department of Aerospace Engineering, Institute of Jet Propulsion, University of the Bundeswehr Munich, Werner-Heisenberg-Weg 39, 85577 Neubiberg, Germany

2 Bundeswehr Technical Center for Aircraft and Aeronautical Equipment, WTD 61, Flugplatz, 85077 Manching, Germany

1 Introduction

The ever-faster development of new technologies and growing global competition are increasing the pressure on companies and engineers to keep up with the current pace of development. At the same time, especially in military aviation, new types of technologies are moving into the focus of the air forces, which have mostly been studied in fundamental research in isolation up to now like hybrid–electric propulsion concepts or fluidic thrust vectoring. The effects of these technologies on the overall system are often relatively unknown and are then investigated in costly and time-consuming demonstrator programs.

This is where the Engine Mission Simulation System (EMSS), developed by the Institute of Jet Propulsion (ISA) in collaboration with Bundeswehr Technical Center 61 in Manching (WTD61), is intended to provide new design capabilities. With a coupled simulation of the aircraft and propulsion system across time-resolved flight missions, a digital, versatile technology demonstrator software has been created that can be used to discover both synergy effects and challenges that still need to be solved. The focus of this research is on the propulsion and power system of fixed-wing aircraft.

The quest for ever more complete simulations of systems in the design phase runs parallel to the increase in available computing power. While the level of detail is constantly increasing in research areas such as high-resolution flow simulation, other researchers are trying to cover a parameter space with simulation in a short time as completely as possible to reduce development time and costs. To date the coupled simulation of aircraft, mission and propulsion is usually limited to two of the three areas aforementioned. For instance, there is extensive research on propulsion–aircraft interaction for hybrid–electric aircraft [1, 2] or the influence of the mission and the propulsion on special subsystems is investigated [3]. Programs for multidisciplinary preliminary design of turbojet engines have been in use for several years [4, 5]. However, the ambition of the Engine Mission Simulation System is a consideration of all three mentioned aspects in sufficient detail with special attention to the propulsion system, without the need of a deep expertise in all areas.

In this paper, first the structure of the designed simulation environment is presented and then the functionality is demonstrated on the basis of an example flight mission for a generic aircraft.

2 Problem definition and methodology

The developed simulation system is supposed to provide time-resolved data of the aircraft and its propulsion system over the flight mission as accurately as possible. For such a

simulation system the highest possible degree of modularity is desirable to be able to exchange individual software modules in the future or even replace them with hardware. To the same degree, emphasis is placed on the extensibility of the environment created, which includes the possibility of automated parametric studies as well as script-based control.

At the same time, a high-performance solution is sought that enables simulations in real time so that pilot-in-the-loop scenarios can be performed in the future.

However, the main requirement for the Engine Mission Simulation System (EMSS) is the ability for co-simulation, avoiding simplifications by surrogate models, especially for the propulsion system. Through this, a higher level of detail as well as a larger data set should be achieved, especially in the overall propulsion and power supply system. Military applications in particular demand fast and dynamic maneuvers that are inadequately represented by approximating them in tabular form or by limiting the simulation to single mission points. Instead, the objective is to achieve the most detailed resolution of the aircraft and propulsion system possible across the entire flight mission.

Taking into account the requirements just mentioned, the Engine Mission Simulation System was realized using external software wherever possible. Section 2.1 first explains the software architecture of the Engine Mission Simulation System. Then, in Sect. 2.2, the individual software used will be discussed.

2.1 Software architecture

The basic structure of EMSS is outlined in Fig. 1, where the software basis of the different substructures of EMSS is color coded. The flight physics, in particular the aerodynamics and flight mechanics of the aircraft, are modeled in X-Plane 11, shown in light blue, while the simulation of the entire physical propulsion system takes place in NPSS®, shown in dark blue. Both the control of the propulsion system, in the conventional case via the fuel quantity as described later, and the flight control as well as the flight guidance are realized in MATLAB®/Simulink®, shown in orange. The data flow between the individual program parts is symbolized by arrows, where dashed arrows stand for Universal Datagram Protocol (UDP) connections, while continuous arrows mean direct signal links in Simulink, respectively, the data exchange between Simulink and NPSS® via the S-function, which will be discussed in more detail later.

The beginning of each computational cycle of EMSS is the calculation of the flight physics in X-Plane 11. The currently acting forces are calculated based on the environmental conditions, the flight attitude and velocity, the positions of the control surfaces and the state and thrust of the engine. In the initial point at $t = 0\,s$, both the flight condition and the state of the controls are user-defined, which, depending
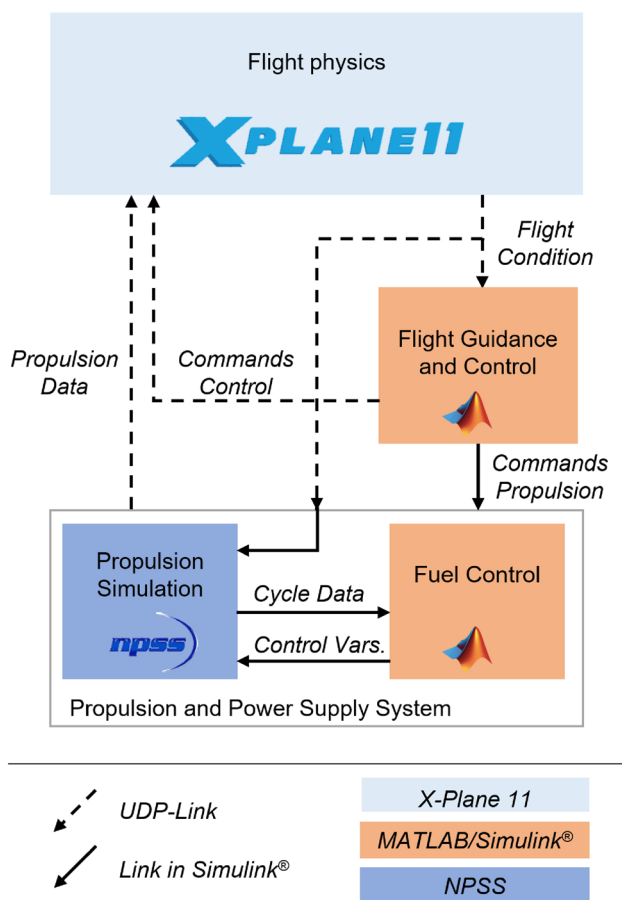
Fig. 1 Program structure of Engine Mission Simulation System

on the input, can correspond to a trimmed or untrimmed flight condition or, as in this case, a stationary situation on the runway. Proceeding from this calculation, the accelerations are derived using the aircraft mass and inertia. The resulting flight condition is not only used as the basis for the next computational step in X-Plane 11, but is also sent

to the flight control system (FCS) in MATLAB®/Simulink® via a UDP connection. Through the flight guidance module, the deviation from the target course is detected, whereupon normalized control surface commands and a thrust lever position are determined based on the flight controllers from Brockhaus [20]. The controller for the longitudinal motion is based on the Total Energy Control System (TECS) ([20], Ch. 17.1.4), while the other controllers and the flight guidance are based on the A320 control system ([20], Ch. 20). The control surface commands are passed to X-Plane 11 for the next computational step while the thrust lever position is further processed in the propulsion and fuel control systems.

There, the thrust lever position $\delta_{T,cmd}$ is converted into a corrected spool speed demand $N1_{c,cmd}$ with the help of a gain factor k_δ as shown in Fig. 2. After checking for violation of limits set as a maximum turbine inlet temperature $T_{041,max}$ or the maximum mechanical spool speed $N1$, the fuel mass flow $\dot{m}_{ff}$ is incrementally increased or decreased under consideration of the maximum step size stp_{max}. Here, both the thermodynamic cycle parameters used to check the limits and the control variables such as the fuel mass flow rate are exchanged between NPSS® and MATLAB®/Simulink® by the S-function. For the first investigations for system functionality validation, this paper focuses on fuel mass flow as the only input variable for a conventional turbofan, which is discussed in further detail in Sect. 3.1. However, there is no strict limit to the number of parameters that are transmitted by the S-function, which currently provides up to ten control variables for the propulsion model.

The performance synthesis model of the propulsion system, which is defined in advance by the user in NPSS®, takes into account not only the input variables from the propulsion and fuel control system, but also the relevant quantities from the flight simulation, such as flight altitude, Mach number or ambient temperature. Taking all these variables into account, the state of the propulsion
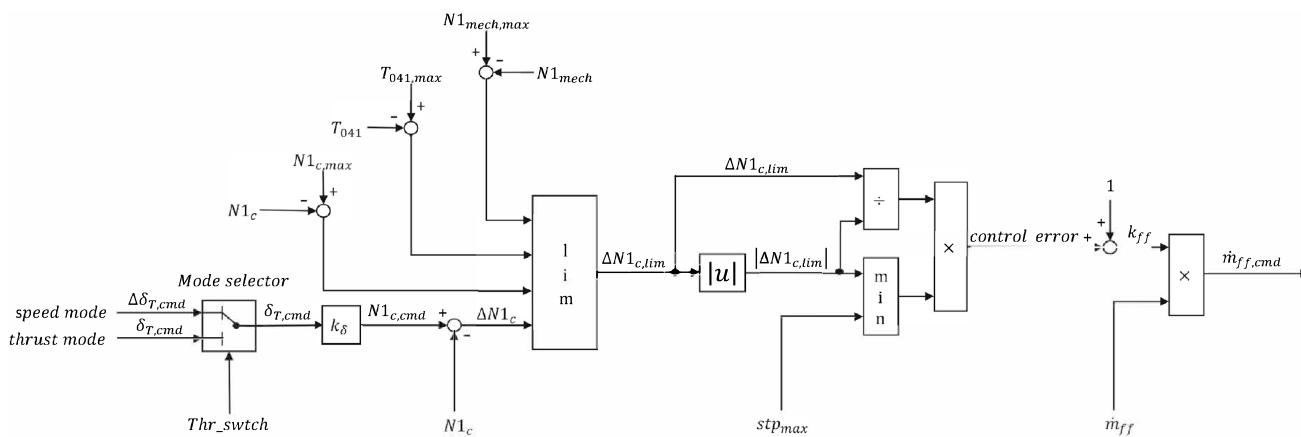

Fig. 2 Discrete fuel controller for the fuel supply in Engine Mission Simulation System

system is determined for the current calculation step and, in particular, the thrust vector and the remaining fuel is forwarded to the flight simulator via the UDP connection. With the updated thrust and the new control commands, the flight physics for the next time step are once again calculated there.

The velocities occurring on the aircraft are determined twice per calculation of the flight dynamics, which in turn are calculated between two and ten times per frame (in this case four times). The data exchange with Simulink can be set as required between 0.1 Hz and 100 Hz. In the present study, a data exchange rate of 20 Hz was selected, to which all other systems are also configured.

In initial investigations, this configuration was found to be stable and sufficiently accurate, even though a careful tuning of the individual time steps to each other is necessary especially for the investigation of transient effects.

2.2 Software used

In the following section, the software used in the Engine Mission Simulation Systemis presented part by part.

2.2.1 NPSS®

In EMSS the propulsion system is modeled utilizing the Numerical Propulsion System Simulation (NPSS®). NPSS® is an object-oriented and multi-physics design and simulation environment that enables development, collaboration, and seamless integration of system models. The main applications of the code, originally developed by NASA (National Aeronautics and Space Administration), are in the performance calculation of aircraft propulsion systems and other thermodynamic analysis [4, 6, 7]. The original version of NPSS® allows only steady-state or transient performance calculation of an engine, as described for example in [8, 9], or [10].

However, an addition of functions is possible both through independent further development that is based on C++, as well as the integration of extensions under free license, such as the Power Systems Library for electrical components [11].

The connectivity of NPSS® to external programs is restricted by its commercial nature and its proprietary nature. Nevertheless the academic version of NPSS® is delivered with a precompiled S-function interface to MATLAB®/Simulink®. In this interface pre-determined parameters are copied from an external program, in this case NPSS®, into MATLAB®/Simulink®. The implementation as an S-function has two major advantages: by transferring the data through the memory, short execution times can be guaranteed, as they are necessary in a co-simulation. At the same time, the integrity of the data is preserved by not having both programs access a shared memory. The suitability of this interface has been demonstrated and validated [12], in particular for the design of engine controllers.

In addition, NPSS® is highly accepted as an industry standard and thus relevant models can be exchanged directly with external partners.

2.2.2 MATLAB/Simulink

Due to the wide distribution and popularity of MATLAB® the user not only has access to many proprietary toolboxes, but also has the possibility to use a lot of open source licensed extensions from scientists and programmers. Of large importance are also the multiple interfaces that MATLAB provides to other languages such as C++ or Python as well as to hardware such as joysticks or microcontrollers, both locally and through diverse network interfaces such as the User Datagram Protocol (UDP). All of this allows a fast implementation of the current requirements and offers many possibilities for extensions of the system in not yet clearly defined directions.

2.2.3 X-Plane 11

The third domain to be simulated is the airframe and its physics. In most scientific applications, pre-calculated flight dynamics models are used, which are then visualized in an external program such as Flight Gear. A first EMSS prototype was also designed in this way. In this case, the flight dynamics models (FDM) can either be outsourced to an external program such as MATLAB/Simulink® [13] or be more or less fully integrated into the flight simulator, such as in Microsoft Flight Simulator or Flightgear via FDM formats such as JSBsim or YASim. However, the creation of such a flight dynamics model requires detailed knowledge of the aircraft to be simulated as well as its aerodynamics, inertia, etc., to derive the corresponding FDM, which is a time-consuming and labor-intensive task.

A different concept of modeling the flight physics of aircraft is followed by the commercial flight simulator X-Plane 11 [14] from Laminar Research under the direction of Austin Meyer. Here, the aerodynamic behavior of the aircraft is not calculated in advance and then provided to the simulator in the form of derivatives. Rather, the aerodynamics and flight behavior of the aircraft are derived from the geometry of the aircraft along with other user inputs and specifications. For this purpose, X-Plane 11 decomposes the aircraft into a number of small elements, for each of which the forces are calculated to subsequently determine the resulting force vector. The entire calculation is based on a refined version of the blade element theory. Taking into account the mass,

the position of the center of gravity and the geometry of the aircraft, velocities, attitude and position can be determined by integrating all force vectors. In X-Plane 11 the physical calculations can be configured to up to 10 computational steps per displayed frame, resulting in a maximum computational frequency of approx. 800Hz on powerful hardware.

For particular aircraft models in combination with certified hardware, X-Plane 11 is approved by the U.S. Federal Aviation Administration (FAA) for pilot training [15]. In recent years, a combination of various versions of X-Plane 11 and MATLAB®/Simulink® has been successfully used by several research groups: mainly for simulating UAVs, their flight control algorithms [16], flight controllers [17], swarm behavior [18] or hardware-in-the-loop [19] simulations.

Furthermore, X-Plane 11 comes with additional programs to design or replicate aircraft for the flight simulator. In PlaneMaker the geometry of the aircraft is specified, while in AirfoilMaker the airfoil polars for the wings and stabilizers can be specified. In addition, an extensive database of aircraft from Laminar Research itself or from the active X-Plane community can be accessed and these aircraft models can be customized as needed.

Based on this, modeling an aircraft for use in X-Plane 11 is possible even for users without expert knowledge in the fields of aircraft design, aircraft aerodynamics or flight mechanics. Instead, an initial aircraft model can be realized within a few working days without the use of elaborate simulations or complex methodologies.

2.3 User interfaces

The Engine Mission Simulation System has several user interfaces, which are discussed hereafter.

2.3.1 Engine definition

The specification of the engine model in NPSS® is text-based, with a syntax similar to C++. Here, each thermodynamic parameter as well as the component maps and the iteration scheme can be adjusted to the user's requirements.

2.3.2 Inlet perturbations

The Institute of Jet Propulsion has been investigating inlet disturbances and their interaction with compressors for several years. To be able to evaluate this interaction and the possible compressor instabilities with regard to the operational behavior of the engine and its performance, an interface was implemented for the simple simulation of inlet distortions with the parallel compressor model [21, 22] directly into the *Propulsion Simulation* in NPSS®. Here,

averaged pressure or temperature distortions can be imposed on one or more compressors and be analyzed over the course of the mission, representing distinguished flight maneuvers.

2.3.3 Flight and propulsion control

Beside the propulsion specific parameters, all flight guidance and flight control parameters can be accessed as well. This means that the flight and propulsion controllers themselves, are fully accessible by the user and can be manipulated at will. Of additional interest is the separated and script-based access to all gain factors within the controllers. This setup enables the controller design itself as well as controller tuning.

2.3.4 Airframe design

One of the biggest motivations to develop EMSS is the investigation of interactions between propulsion system and aircraft design—always under consideration of the entire flight mission. This at least requires adaptability of the key parameters that influence the aircraft, and in the best case even enables the user to design a simple airframe. As already described in Sect. 2.2.3, this may be achieved by included proprietary programs in X-Plane 11, providing an important interface to the engineer to design or manipulate the airframe.

2.3.5 Mission planning

Another important user interface within EMSS is the mission planing interface, which enables a free and yet easy design of flight missions. These missions are built from the predefined sections Waypoint Following, Orbiting, Rolling, Take-Off, Landing, G-Turns, Levelling or Custom. In each of the mission sections, most parameters for the execution, such as flight altitudes, speeds or thrust lever positions, can be chosen freely. The mission assembled from these predefined blocks is then processed in the simulator in stacked order using a state machine.

3 Componentwise verification

In the following section, the simulated components are discussed and a simple validation is carried out on the basis of measured or more detailed simulation data.

3.1 The engine

For the conducted study the Larzac 04 engine serves as a reference for the propulsion model built in NPSS®. The Larzac
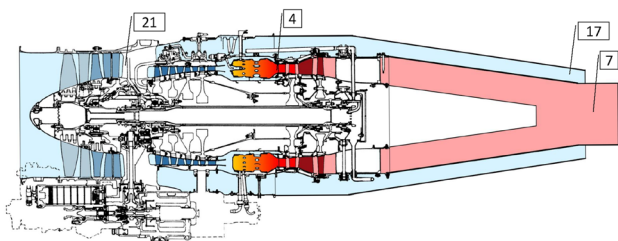
Fig. 3 General arrangement of the Larzac 04C5 engine [23]

Table 1 Engine performance data for the Larzac 04 at Sea Level Standard according to [24]

Technical Data of the Larzac 04	
Net thrust F_N [kN]	13.0
Massflow $\dot{m}$ [kg/s]	27.64
Overall pressure ratio (OPR)	10.4
Bypass ratio BPR	1.13
Burner exit temperature T_{t4} [K]	1403

04 is drawn in Fig. 3 and was developed by the French consortium Groupement Turboméca-SNECMA (GRTS) in the late 1960s and is mainly known as the powerplant of the Franco-German cooperation Alpha-Jet, a twin-engine trainer aircraft and light fighter-bomber for close air support.

The Larzac 04 is a two-shaft, two-stream, afterburnerless engine with a two-stage fan, a four-stage high-pressure compressor, an annular combustor, and a single-stage high-pressure turbine followed by a single-stage low-pressure turbine. The most important parameters of the thermodynamic cycle are listed in Table 1.

The Institute of Jet Propulsion operates Larzac 04 engines as highly instrumented test vehicles at its own engine test facility [25]. The wide set of experimental data from those test vehicles is used to validate the NPSS® model of the Larzac 04, which was set up for the studies presented in this paper. Figure 3 shows a general arrangement of the Larzac 04C5 engine, in which the sample positions used in the study are marked.

Figs. 4 to 6, respectively, show selected points of test data from a low-pressure compressor map measurement and the corresponding results of the NPSS® model for various cycle parameters plotted against the low-pressure shaft speed. The target values for the selection of the calculation points were relative speeds of the low-pressure shaft (54 %, 60 %, 69 %, 76 %, 81 %, 86 %, 90 %, 93 %), which were also used for the measurement of the map.

In Fig. 4, the measured and simulated net thrust at the corresponding power setting, defined by relative spool speed, is plotted. The highest power operating point with a thrust of 12.4 kN can not be run in the test facility and was
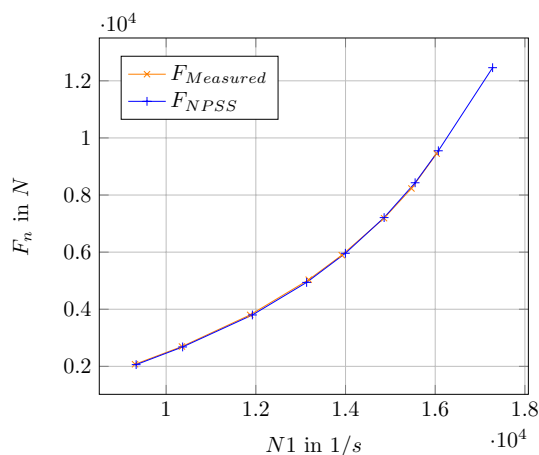

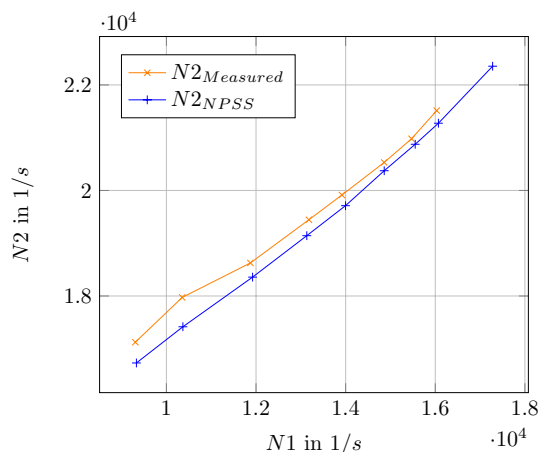**Fig. 4** Thrust curve over the low pressure shaft speed

Fig. 5 High pressure shaft speed above low pressure shaft speed

therefore only simulated. In particular, the good agreement of the two thrust curves of a averaged deviation over all measurements of 0.21% confirms the applicability of the NPSS® model in EMSS.

Nevertheless, for further investigation of the engine model, a validation of further parameters has to be performed. In Fig. 5, the high-pressure shaft speed $N2$ is plotted against the low-pressure shaft speed $N1$. This shows, especially in the part load range, a deviation of −2.30% resp. −3.09% which, though, decreases with increasing load to −0.5% at the penultimate data point, resulting in an average deviation of −1.47%. Some of this deviation is caused by the use of generic maps for the high-pressure compressor and the two turbines in the NPSS® model. The handling bleed, however, accounts for the largest share of the deviation, which will be discussed in more detail later.
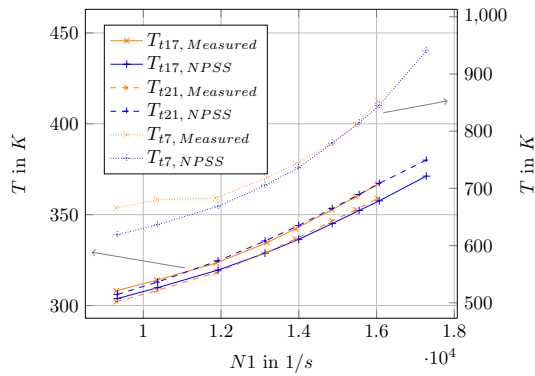
Fig. 6 Total temperature at axial positions 17 and 21 (left axis) and 7 (right axis) above the low-pressure shaft speed

The speed and thus the power of the high-pressure shaft are of particular interest for studies of power and bleed air extraction in the high-pressure part of the engine.

In Fig. 6, the total temperatures at three different axial positions in the engine are plotted against the low-pressure shaft speed. The measured temperatures are mean values of up to six radial measuring positions by up to three temperature sensors in the circumferential direction.

Several observations can be made when looking at the temperature measurements. The total temperature at the end of the bypass stream in the bypass nozzle is underestimated over the entire measured operating range of NPSS®, ranging from 4.3 K at low speeds to 9.2 K at 93% relative rotational speed. This average deviation of T_{t17} by −1.76% can be mainly attributed to negligence of heat transfer in the NPSS® model, which also explains the effect of increasing deviations with increasing temperature gradient to the environment.

The average overestimation of temperature T_{t21} by 1.96% downstream of the low-pressure compressor outlet, in combination with other effects, can probably be attributed to an over-pessimistic efficiency in the NPSS® model.

However, the most obvious deviation is probably seen in the exhaust temperatures in the core stream T_{t7}. Deviations below one percent at higher speed operating points are opposed by an underestimation of the temperature by NPSS® by −6.99% or −6.37% at the measurements with spool speeds below $1.1 \cdot 10^4$ 1/s. Here, the influence of the handling bleed can be observed, which blows off air from above the second high pressure compressor (HPC) stator into the bypass stream under a relative speed of 60 % to stabilize the HPC aerodynamics. Thus, less massflow is delivered to the combustor and turbine section, which in turn demands a higher fuel flow to maintain the power setting of the overall engine, resulting in higher exhaust gas temperatures.
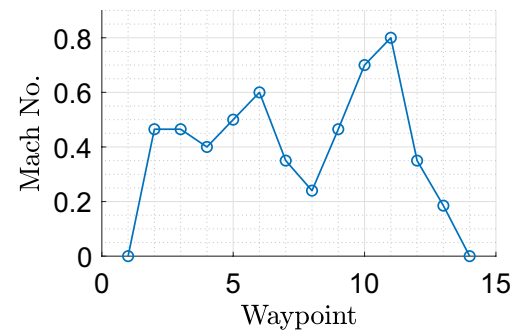
In summary, the NPSS® model replicates the Larzac 04 engine with acceptable deviations. In particular, the small
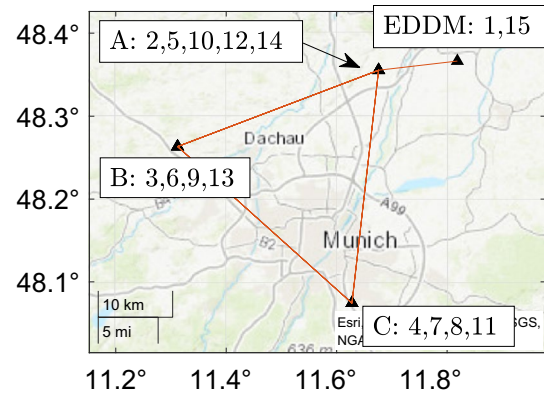
(a) User-defined, numbered waypoints in topographic map
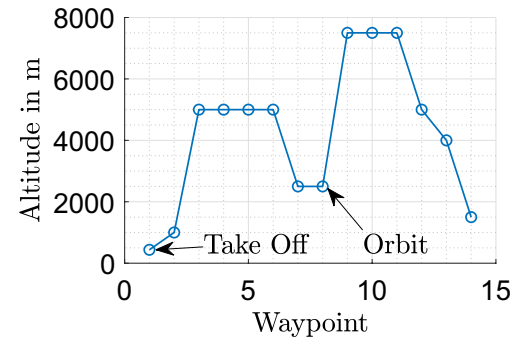
(b) User-defined altitude profile for scenario

(c) User-defined mach number profile for scenario

Fig. 7 Planned mission in a waypoint representation (**a**) with its corresponding commanded altitude profile (**b**) and commanded mach profile (**c**)

deviation in the thrust curve allows the use of the engine model in the Engine Mission Simulation System as a propulsion system.

3.2 The flight mission

The primary task of the Engine Mission Simulation System is the coupled analysis of aircraft and its powertrain within any of its missions. For this purpose, as already explained,

a mission specification is possible by stacking predefined events and additional parameter assignment.

In Fig. 7, the graph on the top (a) shows the predefined flight route from a bird's eye view as the specified waypoints, while the graph on the bottom (c) shows the respective altitude specifications for those waypoints. For simplicity, in the presented mission Munich is circled once at an altitude of 5000 m, then waypoint C in the south is circled twice at 2500 m, after which the return flight is performed at 7500 m through all waypoints until landing in munich airport (EDDM). To demonstrate the principle of the mission guidance, the paper focuses on the three waypoints (WPs) A, B and C in the vicinity of the take-off airport munich (EDDM). Starting from the airport, first A (WP 2) is approached at 1000 m, then all waypoints are passed at 5000 m, whereupon at WP B the descent to 2500 m at C begins. At WP 8, the aircraft circles around C. The return flight follows the same pattern at 7500 m until the signal of the instrument landing system (ILS) is intercepted at WP 14, which initiates the automatic landing procedure. In the lower part of the mission, an acceleration from Mach 0.4 to Mach 0.6 is performed, while the return flight is flown between Mach 0.7 and Mach 0.8, as shown in the middle graph (b).

The mission replicates the main elements of a real mission, but it is not to be understood as such, since it is intended solely as a generic example for verifying the functionality of EMSS.

3.3 The airframe

To be able to demonstrate the functionality of EMSS for the presented paper, an aircraft model is necessary, which has to fulfill some requirements. In general, the type and size of the aircraft must be suitable for the intended mission. In its research on the overall system, the Institute of Jet Propulsion focuses on propulsion systems of the lower and medium thrust class, as they can be investigated in the institute's own test facility and are predestined for unmanned aerial vehicles. A potential mission of such a system is described in more detail in Sect. 3.2. In addition, the flight vehicle and the propulsion system have to be matched. Although this would also be possible by scaling the propulsion system, either in its entirety or only the thrust and the SFC, in the present case a weight of 1800 kg to 2100 kg leads to a typical thrust-to-weight ratio of 0.6−0.7 of the flight vehicle, equipped with the Larzac 04 as the propulsion system. At the same time, aerodynamic stability of the aircraft is required, as well as favourable flight characteristics, even under the influence of light disturbances. For simplification of the first study, a purely subsonic design will be considered initially.

Based on the requirements just mentioned, the Airbus Do-DT 25 target display drone [26] was chosen as the conceptual basis of the principal aircraft architecture for
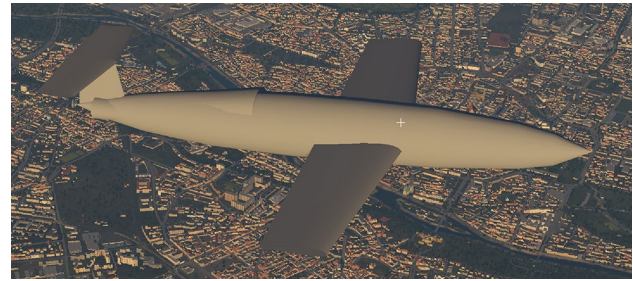

Fig. 8 Graphical modeling of the Unmanned Propulsion and Energy Research Aircraft in X-Plane 11 as used for the studies in this article

Table 2 Technical data of Unmanned Propulsion and Energy Research Aircraft

Technical data of UPERA	
MTOW [kg]	2100
Operating Empty Weight (OEW) [kg]	1500
Span [m]	6.0
Wingloading [kg/m²]	187.5

this investigation, but its size, with a maximum takeoff mass of 144 kg, does not meet the requirements. The designed flying system UPERA (Unmanned Propulsion and Energy Research Aircraft) in Fig. 8 was designed to have a configuration as the target demonstrators Do-DT 25, but was upscaled such that it has an MTOW of 2100 kg, 14.6 times the maximum weight, and with 7 m length and 6 m wingspan, more than double the dimensions of the target display drone. Further important technical data can be found in Table 2.

To evaluate the quality of the modeling of self-created flying objects in X-Plane 11, a computer-aided design (CAD) model of the aircraft was examined with respect to its aerodynamic behavior using the CATIA v5 plug-in FloEFD. FloEFD from Siemens [27] is a flow solver based on the finite volume method, using the immersed-boundary method. The Reynolds-averaged Navier–Stokes equations are closed from FloEFD by the k-ϵ-turbulence model. The modified wall functions uses a van Driest profile for the wall near region. For mesh cells in wall proximity bigger than the boundary layer thickness, integral boundary layer theory is applied [27].

Besides the integration of the flow solver into CATIA, its auto-meshing also enhances its user-friendliness. The automatically generated ordered rectangular mesh was gradually refined by inputs both at the solid boundaries and in domains of particular interest. A brief mesh convergence study resulted in approximately 31 million cells for the studies conducted on the described aircraft, which is assumed to provide results with sufficient accuracy for the present study.

Table 3 Boundary conditions, target variables and deviations of the aircraft model between X-Plane 11 and the flow solver FloEFD

Boundary Conditions

Calculation Point	1	2	3	4	5
$Alt_{MSL} [m]$	7500	5000	5000	2500	1800
$p_\infty [kPa]$	38.30	54.05	54.05	74.69	81.40
Ma_∞	0.75	0.60	0.50	0.50	0.40
$\alpha_\infty [deg]$	0.70	0.70	2.20	1.05	2.69
Target Variables					
$F_{Lift,xPlane} [kN]$	26.24	22.40	22.23	22.12	22.19
$F_{Drag,xPlane} [kN]$	2.14	1.61	1.39	1.55	1.40
$F_{Lift,CFD} [kN]$	23.74	18.01	19.44	18.34	20.81
$F_{Drag,CFD} [kN]$	2.09	1.62	1.47	1.56	1.50
$\Delta F_{Lift} [\%]$	1.42	23.84	14.35	20.61	6.63
$\Delta F_{Drag} [\%]$	2.39	−0.62	−4.76	−0.64	−6.67

Fig. 9 Specific Fuel Consumption in kg/(N s) over the overall pressure ratio for various bypass ratios

In the upper part of Table 3 the considered flight conditions are listed, which at the same time represent the boundary conditions for the corresponding CFD calculation. In addition, the symmetry of the aircraft in its central axis was utilized due to the flow conditions without slip angle, while engine effects were not taken into account.

The calculation points with the different flight altitudes up to 7500 m and flight Mach numbers up to 0.75 represent the envelope of the investigated aircraft. The data from X-Plane 11 are taken from level flight situations. Since the drag of the airplane is of primary interest for the investigation of the propulsion system, the discussion is focused on a comparison of the latter.

In calculation point 1 the drag of the aircraft is slightly overestimated by X-Plane 11. This can be explained, inter alia, by the use of Prandtl–Glauert corrections to account for compressibility effects and an empirical correlation for mach-divergent drag increase by X-Plane 11.

The deviation in the calculation points 2 and 4 is below 1%, while the deviation in point 3 is 4.8% and in point 5 6.7%. Here a correlation with the angle of attack becomes evident: with increasing angle of attack the deviation between CFD and X-Plane 11 grows.

These results are all within a maximum deviation of 10%. Despite the sufficient agreement in the present case, further investigations should be carried out in the future.

4 Parametric study

This subsection is intended to demonstrate a typical workflow for a design variation of a propulsion system with EMSS. To demonstrate this capability of the Engine Mission Simulation System, a parametric study was conducted based
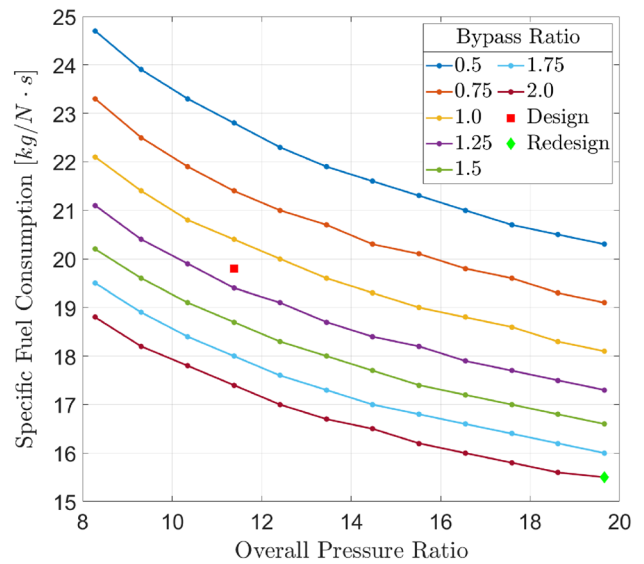
on the Larzac 04 engine introduced in Sect. 3.1. Based on this study, the engine variant with the lowest specific fuel consumption was selected and used as the propulsion model for the mission presented in Sect. 3.2 and compared to the original propulsion model.
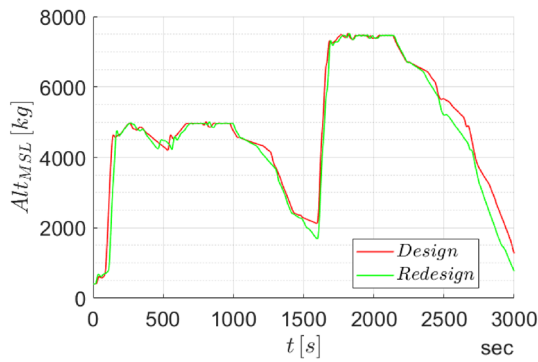
The exemplary target parameter of this study on the mission impact on two different engine configurations is fuel consumption.
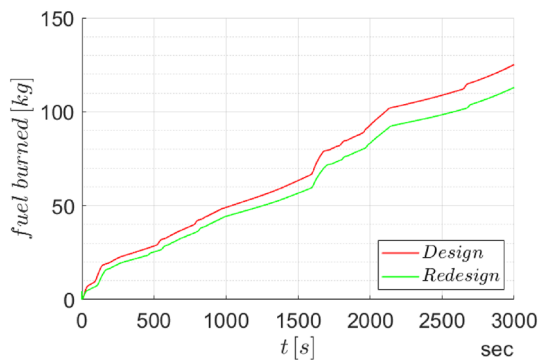
4.1 Engine standalone

For this purpose, starting from the reference design point with a BPR of 1.16 and an OPR of 11.22, the bypass ratio was varied from 0.5 to 2. In this process, the ratio of the exit velocities of the inner and outer nozzle was kept constant by adjusting the inner and outer fan pressure ratios accordingly. At the same time, the ideal overall pressure ratio was varied from 9 to 20. At constant temperature at the combustor outlet, all engines in the parametric study meet the same thrust requirement through differing design mass flow rates.

In Fig. 9, the specific fuel consumption of all designed engines is plotted against the bypass ratio at the corresponding overall pressure ratios. As expected, the specific fuel consumption decreases with higher bypass ratios due to the increasing mass flow as the jet velocity decreases. The same effect is observed with increasing pressure ratio.

With this study the possibility for parametric design studies within EMSS is demonstrated as an early step in the pre-design of propulsion systems.
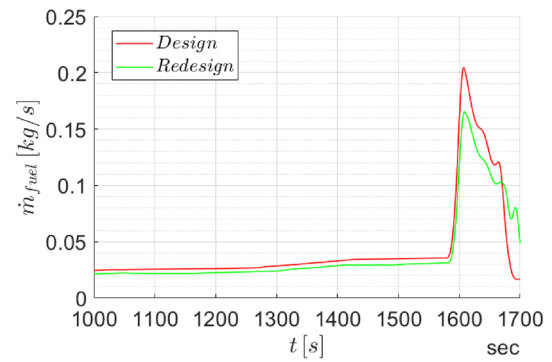
(a) Flight altitude [m]

(a) Fuel mass flow rate [kg/s]

(b) Burned fuel mass [kg]

(b) Combustor exit temperature [K]

Fig. 10 Development of the flight altitude above sea level [m] (**a**) and the total fuel mass burned [kg] (**b**) over the duration of the mission
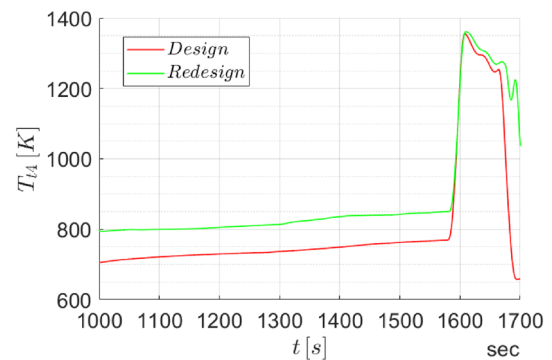
Fig. 11 Fuel mass flow rate $\dot{m}_{fuel}$ and the combustor exit temperature T_{t4} over a section of the mission progress

4.2 Engine and airframe in their flight mission

For the results in this subsection, the mission described in Sect. 3.2 was simulated with the two engines selected in the previous section. The original configuration (BPR = 1.16, OPR = 11.22) always drawn in red and the redesigned engine (BPR = 2, OPR = 19.66) in green. The selected data is intended to demonstrate capabilities and possible applications of EMSS.

In Fig. 10 the altitude profile above sea level (a) and the development of the burned fuel mass (b) throughout the mission are shown. With the help of the altitude profile, consistency with the specified mission planning can be confirmed, although a certain transient response can be observed, especially during the acceleration processes at an actually constant altitude. In the comparison between altitude profile and burned fuel, the higher fuel consumption during the climbs becomes obvious. It is of interest that the configuration with redesigned engine only achieved approx. 9.8% fuel savings compared to the

baseline configuration, although the SFC differs by 22.5% in the engine standalone case.

One reason for this can be found in Fig. 11. Despite the same combustion chamber outlet temperature T_{t4} at the design point, the temperature difference at part load operation amounts to approx. 70K at the expense of the new design, which reduces the difference in fuel mass flow between the two propulsion options in the same mission section to approx. 15%.

Results like this, which can only be obtained by looking at the entire mission, are the added value of a fully parallel simulation like the one performed in EMSS.

5 Conclusion and outlook

This paper presents the architecture and the functionalities of a combined aircraft and propulsion simulation, called Engine Mission Simulation System (EMSS). After an introduction of the system architecture and the software used, the

engine model was validated and the aerodynamics of the aircraft was verified. In both cases, a good agreement of the models with the experiment and a higher-order simulation could be shown. Subsequently, a parametric study of the engine was carried out, using the most fuel-efficient resulting engine to simulate an exemplary flight mission in EMSS. The comparison of those two identical missions with the same aircraft but different engines shows a much lower fuel saving over the mission than a pure consideration of the SFC would suggest.

Even though the influence of the coupled system can already be clearly shown here, there are still some uncertainties in the Engine Mission Simulation System. For example, the influence of flight controllers that are not matched to the respective application on the particular aircraft–propulsion combination must be investigated in more detail. In addition, no optimization of the aircraft and propulsion system has yet been carried out in the study presented here, which also reduces the validity of the results.

Nevertheless, generally the effects of certain propulsion system characteristics on the flying system can be determined and evaluated, based on such mission-resolved outcomes. Especially in the case of highly mission-dependent systems such as electro-hybrid propulsion systems with buffer storage or in the case of more complex missions such as in the defence sector, a deeper knowledge of the influence of the mission design on the propulsion system is advantageous. Likewise, in the case of additional requirements on the propulsion and power system, such as the short-term demand of large electrical powers, a consideration within the mission is essential to avoid an oversized design and still fulfill all requirements. Likewise, the effects of flight condition-specific disturbances on the safe operation of the engine's compressor while providing sufficient performance by the presented system can be investigated. By knowing about all relevant flow parameters and thermodynamics, it would also be possible to evaluate maneuvers in regard to their thermal and abrasive degradation of the propulsion components.

In summary, the time-resolved simulation will provide a better understanding of the propulsion and power system, which will allow a more tailored design for each specific application.

Declarations

References

1. Zhang, Jinning, Roumeliotis, Ioannis, Zolotas, Argyrios: Model-based fully coupled propulsion-aerodynamics optimization for hybrid electric aircraft energy management strategy. Energy **245**, 123239 (2022). https://doi.org/10.1016/j.energy.2022.123239

2. Dean, Tyler S., Wroblewski, Gabrielle E., Ansell, Phillip J.: Mission Analysis and Component-Level Sensitivity Study of Hybrid-Electric General-Aviation Propulsion Systems. J. Aircraft **55**(6), 2454–2465 (2018). https://doi.org/10.2514/1.C034635

3. Allison, Darcy L., Alyanak, Edward J., Shimmin, Kyle: Aircraft System Effects Including Propulsion and Air Cycle Machine Coupled Interactions. In *AIAA SciTech*, San Diego, California. American Institute of Aeronautics and Astronautics. (2016). https://doi.org/10.2514/6.2016-0671

4. Claus, R. W., Evans, A. L., Follen, G.: Multidisciplinary propulsion simulation using NPSS. In *4th Symposium on Multidisciplinary Analysis and Optimization*, Reston, Virigina. American Institute of Aeronautics and Astronautics. (1992). https://doi.org/10.2514/6.1992-4709

5. Schaber, Reinhold: *Numerische Auslegung und Simulation von Gasturbinen*. Dissertation, Technische Universität München, München, (2000)

6. Claus, R.W., Evans, A.L., Lylte, J.K., Nichols, L.D.: Numerical propulsion system simulation. Comput. Syst. Eng. **2**(4), 357–364 (1991). https://doi.org/10.1016/0956-0521(91)90003-N

7. Ransom, David L.: About Numerical Propulsion System Simulation® (NPSS®). Technical report, Southwest Research Institute® (SwRI®), Mechanical Engineering Division, Machinery Department, (2020)

8. Carter, Richard E., Smith, Brian M.: The Development of an NPSS Engine Cycle Model to Match Engine Cycle Data, Using a Multi-Design-Point Method. In AIAA Scitech,: Forum, Reston, Virginia, 01112021. American Institute of Aeronautics and Astronautics (2021). https://doi.org/10.2514/6.2021-0876

9. Nelson-Weiss: NPSS Introduction Webinar. Technical report, Southwest Research Institute® (SwRI®), Mechanical Engineering Division, Propulsion & Energy Machinery, (2022)

10. Rick, Hans: *Gasturbinen und Flugantriebe*. Springer Berlin Heidelberg, Berlin, Heidelberg, (2013). https://doi.org/10.1007/978-3-540-79446-2

11. Csank, Jeffrey, Sadey, David J., Lavelle, Thomas M., Garcia, Jesus, Bergeson, Jennifer, Sizing: Electrical Power System within the Numerical Propulsion System Simulation. In,: AIAA/IEEE Electric Aircraft Technologies Symposium (EATS), Piscataway, NJ, 2019. IEEE (2019). https://doi.org/10.2514/6.2019-4183

12. Chin, Jeffrey C., Csank, Jeffrey T., Haller, William J., Seidel, Jonathan A.: *An introduction to transient engine applications using the numerical propulsion system simulation (NPSS) and MATLAB*. (2016)

13. Hansen, Ole: *Development of a Simulation Environment for Parametric Analysis of Engine Concepts in the Context of a Flight Mission*. Master thesis, Universität der Bundeswehr, München, (2021)

14. Laminar Research. X-Plane 11 Flight Simulator - More Powerful., 2020-09-23

15. Laminar Research. 2023-08-17 FAA-Certified X-Plane. https://www.x-plane.com/pro/certified/

16. Bittar, Adriano, Figueiredo, Helosman, Guimaraes, Poliana Avelar, Mendes. Guidance, Alessandro Correa: Software-in-The-Loop Simulation Using X-Plane and Simulink for UAVs: 2014 International Conference on Unmanned Aircraft Systems (ICUAS). (2014)

17. Bittar, Adriano: Experimental Framework for Evaluation of Guidance and Control Algorithms for UAVs: 21st Brazilian Congress of Mechanical Engineering. *Proceedings of CODEM 2011*, (2011)

18. Garcia, Richard, Barnes, Laura: Multi-UAV simulator utilizing X-plane. J. Intell. Robot. Syst. **57**(1–4), 393–406 (2010). https://doi.org/10.1007/s10846-009-9372-4

19. Bittar, Adriano, de Oliveira, Neusa Maria Franco, de Figueiredo, Helosman Valente: Hardware-In-the-Loop Simulation with X-Plane of Attitude Control of a SUAV Exploring Atmospheric Conditions. *Journal of Intelligent & Robotic Systems*, 73(1-4):271–287, (2014). https://doi.org/10.1007/s10846-013-9905-8

20. Brockhaus, Rudolf, Alles, Wolfgang, Luckner, Robert: *Flugregelung*. Springer Berlin Heidelberg, Berlin, Heidelberg, (2011). https://doi.org/10.1007/978-3-642-01443-7

21. Cousins, William T., Davis, Milt W.: Evaluating Complex Inlet Distortion With a Parallel Compressor Model: Part 1—Concepts, Theory, Extensions, and Limitations. pages 1–12. American Society of Mechanical Engineers Digital Collection, (2012). https://doi.org/10.1115/GT2011-45067

22. Kurzke, Joachim: Effects of Inlet Flow Distortion on the Performance of Aircraft Gas Turbines. *J. Eng. Gas Turbines Power*, 130(4), (2008). https://doi.org/10.1115/1.2901190

23. Kern, Felix: Erkennung und Vermeidung von Verdichterinstabilitäten am Turbostrahltriebwerk Larzac 04 Dissertation. Universität der Bundeswehr München, Neubiberg (2022)

24. der Luftwaffe, Führungsstab: GAF TO 2J-Larzac-02: 10. Änderung: German Airforce Technical Order. Technical report, (02.05.1989)

25. Bindl, Stefan, Muth, Bastian, Niehuis, Reinhard: Experimental Investigations on Macro-Aerodynamics Within a Jet Engine Ground Test Facility: American Institute of Aeronautics and Astronautics. AIAA (2009). https://doi.org/10.2514/6.2009-4828

26. Airbus TS&S. Target Systems & Services by Airbus Defence and Space. (2021)

27. Mentor Graphics Corporation. FloEFD Technical Reference: Software Version 17. Technical report, (2018)